

Dam break modeling and downstream flood inundation mapping on Darbandikhan Dam, Iraq

 Isam Dhahir Khudhur^{1*},  Ahmed N. A. Hamdan²

^{1,2}Civil Department, College of Engineering, University of Basrah, Basrah, Iraq; esam_civil@yahoo.com (I.D.K.).

Abstract: It is important to consider the catastrophic effects of dam collapses to make emergency and evacuation plans. This study simulates the hypothetical collapse of the Darbandikhan Dam in northeastern Iraq. Then, it routes the resulting flood from this collapse to the downstream region with an approximate length of 325 km. The flood impact was analyzed using the 2D HEC-RAS model with the help of ArcGIS software. The outflow peak discharge of the breach at the dam site reached approximately 381.1×10^3 m³/s. Inundation maps were created using RAS-Mapper, which contains the flood wave's depth, velocity, and arrival time distribution through the study area. The maximum values of depth and velocity were (17.5-58) m and (2-22) m/s, respectively, in Sirwan district near the dam, with an arrival time (0.13-0.6) hr. The minimum values of depth and velocity were in the Al-Aziziyah district, which is located at the farthest point from the dam in the study area, which were (0-0.6) m and (0-0.3) m/s, respectively, with an arrival time of (169-186) hr. It is hoped that this research will contribute through its results to providing valuable data to enhance emergency preparedness and effective evacuation planning in the event of a dam failure.

Keywords: Darbandikhan Dam, Dam collapse, Inundation map, Peak discharge, The flood wave.

1. Introduction

There are necessary benefits that are provided to society by dam construction, such as water supply, irrigation, recreation, electrical power generation, and flood control. However, there is a possibility of catastrophic floods occurring due to the collapse of these dams and the escape of the trapped water into the river downstream of the dam through the breach. The size of the flow is different compared to all previous floods and is much larger, and the response time available for warning cannot be compared with the time of precipitation-runoff floods as it is much shorter [1]. There are many features in which the flood resulting from the collapse of dams differs from other types of floods, such as its immediate occurrence, the presence of a large amount of flow, and progress with a powerful force. Some factors affect the process of propagation of the flood resulting from a dam break, such as the types of failure, slope stability, the shape of the dam, sediment transport, and hydrological and hydraulic data that are related to the downstream area [2]. Earthen dams can be considered among the most widely constructed dams around the world because of their low cost and also because they are better suited for construction under different geomorphological and geological conditions compared to other types of dams [3]. However, earthen dams are considered the most vulnerable to collapse because they are less rigid [4]. There are various reasons for breaching the dam, including natural disasters such as heavy rainfall, earthquakes, and landslides. There are also factors caused by humans, such as poor maintenance, design defects, construction errors, or deliberate destruction of the dam by the enemy [5-7]. The collapse of a dam may result in massive flood waves that lead to catastrophic damage and, consequently, Severe property destruction or human fatalities occurring downstream of the dam. More than 450 notable dam collapses were recorded around the world between 2000 and 2019, resulting in deaths and major economic losses [8, 9]. Hydrological and hydraulic models are the primary techniques employed for flood routing. The hydrological routing method utilizes the continuity equation to

generate an attenuated hydrograph of floods at a certain site. However, it cannot offer precise data on surface water elevation and flow velocity.

In contrast, hydraulic routing is used in most dam-break problems, where it solves the continuity and momentum equations. Therefore, it can be considered an alternative and more appropriate approach for simulating the result of a flood wave from a dam failure [10]. Several models can calculate the process of flood routing, which are one-dimensional (1D), two-dimensional (2D), or 1D-2D [11]. Many models or software are used to analyze dam failure, and they are also used in the investigation of propagation of flood waves downstream of the dam. The most important and widely used software is the Hydrological Engineering Center - River Analysis System (HEC-RAS), which the Hydrological Engineering Center of the US Army Corps of Engineers developed. HEC-RAS can solve problems related to floods; it can calculate breach parameters of dams, analyze river flow, as well as draw inundation maps and hydraulic simulations of flood waves. Thus, it is widely used for this purpose [12-17].

Many studies have addressed the issue of dam collapse, including Haltas et al. (2016) conducted a study dealing with predicting the flood wave that occurs after the collapse of the dam in a densely populated downstream area, using both the HEC-RAS and GIS software and analyzing the spread of the flood wave downstream. The study was carried out on Porsuk Dam and Alibey Dam in Turkey [18]. Mao et al. (2017) developed a management system for mapping dam collapse risks in the complex basin environment by analyzing flood routing under the most dangerous scenarios, taking the Foziling Reservoir in China as a case study, and using the Mike 21 software [2]. Mani et al. (2020) simulated different types of floods that led to the hypothetical collapse of the Dhauliganga Dam in India, where the hydraulic model was developed using the Mike 11 software. The development of the breach in the dam section was modelled, and the breach outflow discharge was computed, followed by the routing of the flood hydrograph downstream [19]. Al-Taiee and Mustafa (2020) applied the hydrodynamic model (IBER) to Model the water flood caused by the theoretical collapse. of the Mosul Dam in Iraq by using several storage scenarios after performing the validity test and calibration of the model to identify the inundated areas from the dam site to south Mosul City [20]. Karim et al. (2021) used the 2D HEC-RAS model to simulate the flood wave caused by the hypothetical collapse of the Al-Udhaim Dam in Iraq, as well as analyze the spread of the flood wave along a length of 100 km below the dam site, where the severity of the potential collapse of the Al-Udhaim Dam was deduced [21]. Tedla et al. (2021) mapped Inundations caused by the theoretical breach of the Kesem embankment dam in Ethiopia by coupling both HEC-RAS and HEC-HMS systems based on varying return durations of flood inflow (50,100, and 200) years return period inflows. A two-dimensional, unsteady flow hydrodynamic model was used to simulate dam failure [22]. Riswal et al. (2022) conducted a study in which the impact of the floods resulting from the collapse of the Karalloe dam in Indonesia was analyzed using the two-dimensional HEC-RAS and GIS software. They relied on rainfall data to calculate the results of design flood discharge [23].

Research is being conducted in the hypothetical collapse field of dams and simulation of the resulting floods to assess the potential risks that follow. As a result, all preventive plans can be made, and warning systems can be developed by local governments in preparation for emergencies as a means of assuring the safety of communities situated downstream of the dam and close to the river. Accordingly, this research was conducted to simulate the floods resulting from the hypothetical collapse of the Darbandikhan Dam, identify the places exposed to the flood wave, which are located in the area of the mouth of the Diyala River (Sirwan), and the impact of the spread of the flood wave on those places, such as knowing the values of depths, velocities, and arrival time of the flood wave. This research contributes to providing the data required to enhance emergency preparedness and effective evacuation planning in the event of a dam failure (God forbid). The results can help decision-makers and emergency response teams assess risks and plan infrastructure to reduce loss of life and property; this confirms the importance of the study in practical applications and decision-making.

2. The Study Area

The study area is located in part of Diyala Governorate and small parts of Al-Sulaymaniyah, Baghdad, and Wasit. It extends from Lake Darbandikhan in northeastern Iraq until it meets the Tigris River in southern Baghdad. It is bordered to the north by Al-Sulaymaniyah Governorate, to the west by Salah al-Din and Baghdad Governorates, to the south by Wasit Governorate, and to the east it is bordered by the rest of Diyala Governorate [24]. The Diyala River Basin, in general, includes the Diyala River in addition to all the tributaries that feed it; the catchment area is located in the Iraqi and Iranian lands. The Diyala River Basin is considered one of the important basins in Iraq as it is considered an important nutrient for the Tigris River at an annual rate of (4.3 tons per cubic meter), which is approximately 17% of the total flow of the Tigris River. As for the lines of longitude and latitude, it is located between ($33^{\circ}4'59'' - 35^{\circ}49'58''\text{N}$ and $44^{\circ}30'00'' - 46^{\circ}49'58''\text{E}$) for the study area with all its tributaries [24-26]. Figure 1 shows the location of the study area. The study area consists of two upper and lower parts. The upper part extends from Lake Darbandikhan in Sulaymaniyah Governorate to Lake Hemrin in Diyala Governorate. In contrast, the lower part extends from Lake Hemrin to the Tigris River near Baghdad city.

The impact of the flood resulting from the collapse of the Darbandikhan Dam will be studied for the vital cities in the study area, which are the cities of Darbandikhan, Sirwan, Kalar, Khanaqin, Jalawla, and Saadiya in the upper part. And the cities of Al-Muqdadiah, Khalis, Baqubah, Baladrooz, Kanaan, and the regions of Baghdad, east of the Tigris, all the way to the city of Al-Aziziyah, north of Wasit Governorate, towards the south.

Darbandikhan Dam is the dam located on the Diyala (Sirwan) River, which is considered one of the most important tributaries of the Tigris River, to form a lake known as Darbandikhan. It is located in the Sulaymaniyah Governorate, about 65 km southeast of the city, while 285 km northeast of the capital (Baghdad), about 20 km from the Iraqi-Iranian border ($35^{\circ}06'46''\text{N}$ & $45^{\circ}42'23''\text{E}$).

Hemrin Dam, a dam located within the study area i.e., the inundation area, is an embankment dam. It is on the Diyala River, considered a significant tributary of the Tigris River to form Hemrin Lake. Its location is in Diyala Governorate, 120 km northeast of the capital, Baghdad [27]. After the 1974 flood, it was noted that it was necessary to construct the Hemrin Dam to control river floods. The first studies were conducted, and then work began to complete the dam construction (1974-1981). It is considered one of the strategic projects within the Diyala River Basin [28, 29].

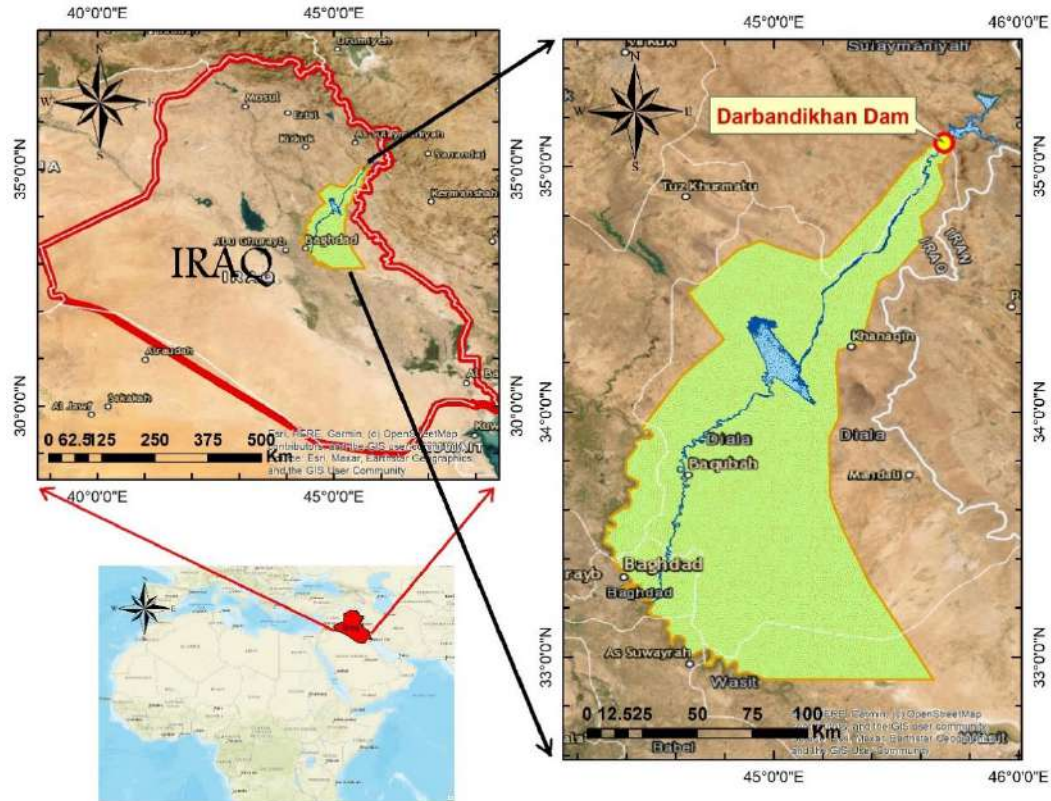


Figure 1.
The location of study area.

3. Materials and Methods

3.1. The mathematical Model

This research idea is based on simulating the hypothetical collapse of Darbandikhan Dam and analyzing the potential effects of floods resulting from this event in the downstream area. Hydraulic modelling was used through the HEC-RAS software version 6.0 to create a 2D unsteady mathematical model due to the ability of this software to simulate the hydraulics of water flow through natural rivers. The HEC-RAS software calculates the water flow hydraulic properties, represented by depths, velocities, etc. HEC-RAS relies on the implicit finite volume method as a numerical solution to solve the continuity and momentum equations [30]. The implicit finite volume solution is mainly used in computational fluid dynamics. In addition to the HEC-RAS software, Geographic Information Systems (GIS) were used to prepare the necessary topographic data used in the mathematical model to draw a terrain map of the study area, which helps in visualizing and analyzing the spread of the flood. Figure 2 represents the HEC-RAS main menu in version 6.0.

The HEC-RAS software uses the input data of dam characteristics and the reservoir to analyze the dam failure, predict the breach opening, and then calculate the breach outflow discharge hydrograph. Then, it uses the breach outflow discharge hydrograph as the upstream boundary conditions to simulate floods in the downstream area that result from the dam break. The above process is done to calculate the flood hydraulic characteristics.

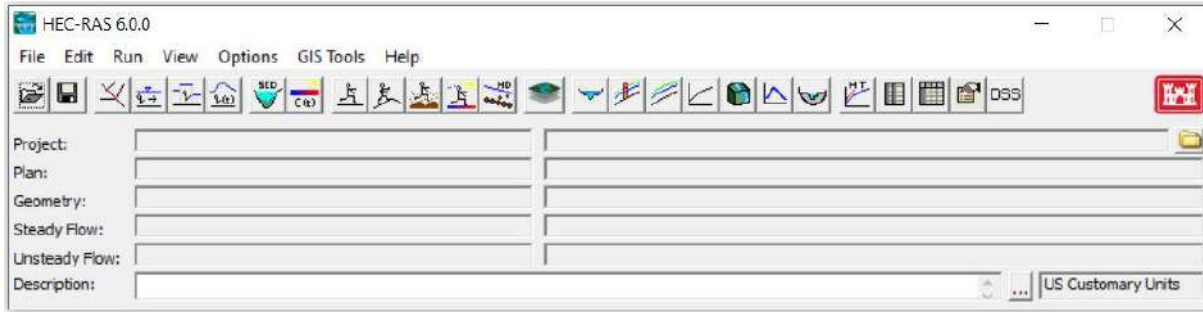


Figure 2.
The HEC-RAS 6.0 main menu.

3.2. Description of Darbandikhan Dam

Darbandikhan Dam is a fill dam with rocks with a central clay core including filter layers, with a height of 128 m, length of 535 m, crest elevation of 495 meters above sea level, crest width of 17 m, both upstream-downstream side slope of 1.75H:1V, and reservoir volume at normal operation level 3×10^9 m³. It has multiple purposes, such as Flood control, storing and providing water for a variety of uses, Electrical Power Generation, and tourism [28]. There are more details in Figure 3 which represents the cross-section of the Darbandikhan Dam.

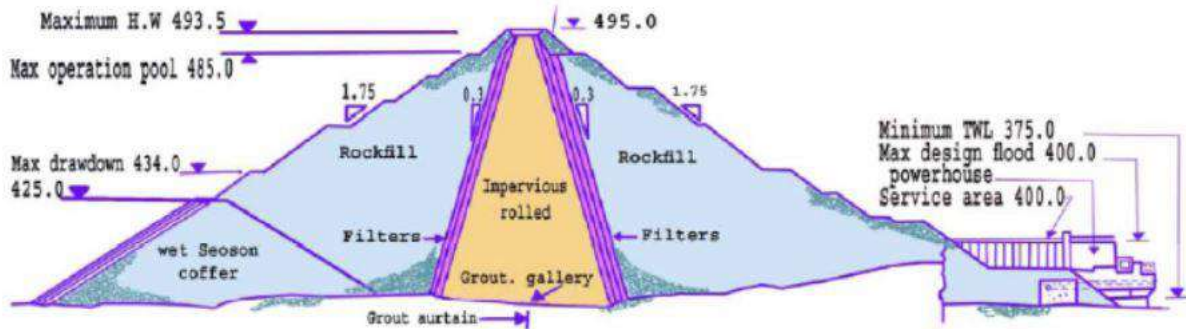


Figure 3.
Darbandikhan Dam cross-section [28].

3.3. Land Surface Data of the Study Area

3.3.1. Digital Elevation Model

The Digital Elevation Model (DEM) was used in this research with a resolution of 12.5 x 12.5 m and in GeoTIFF format. It was obtained from the instrument (PALSAR), which is on the Advanced Land Observing Satellite (ALOS) of the Alaska Satellite Facility (ASF), <https://search.asf.alaska.edu/>. There are many freely available DEMs, but the DEM of ALOS PALSAR – ASF is finer spatial resolution. Due to the large area of the study, 21 clips of DEM images were uploaded and then processed through ArcGIS software (version 10.5). The images of DEM were merged into one image containing the entire study area and surrounding areas through the mosaic process in the ArcGIS software, as shown in Figure 4. The final DEM was imported to the HEC-RAS software to transfer it to the digital terrain model (DTM) for use in the simulation process, where the digitization of the 2D grid flow and storage area was done, as shown in Figure 5.

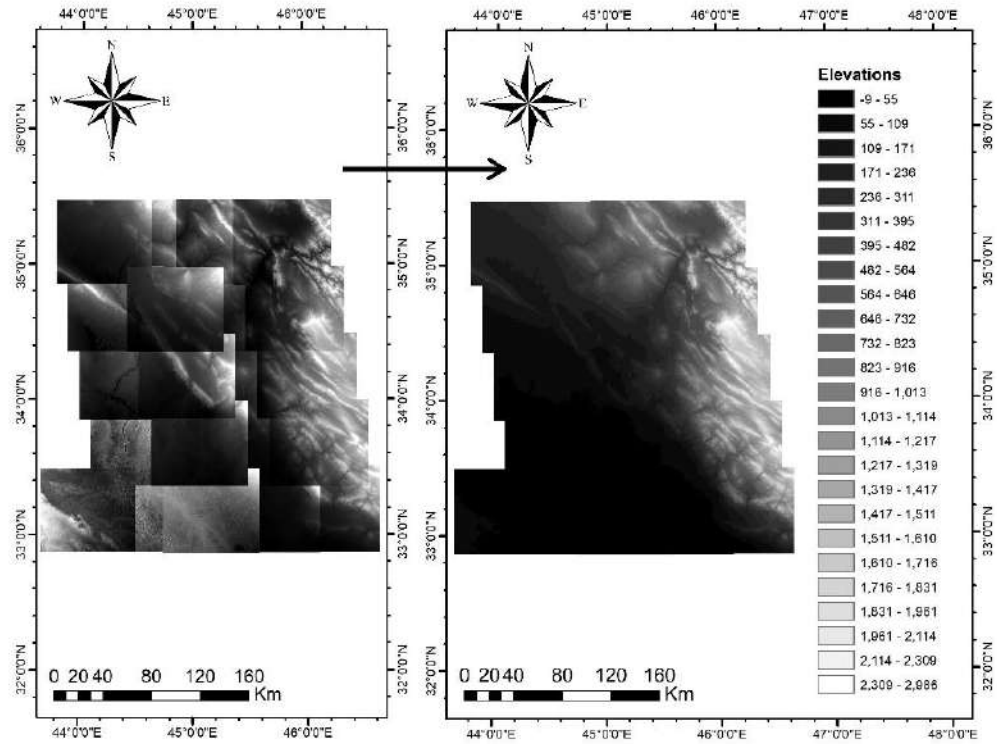


Figure 4.
Digital elevation model (DEM) of Diyala River Basin.

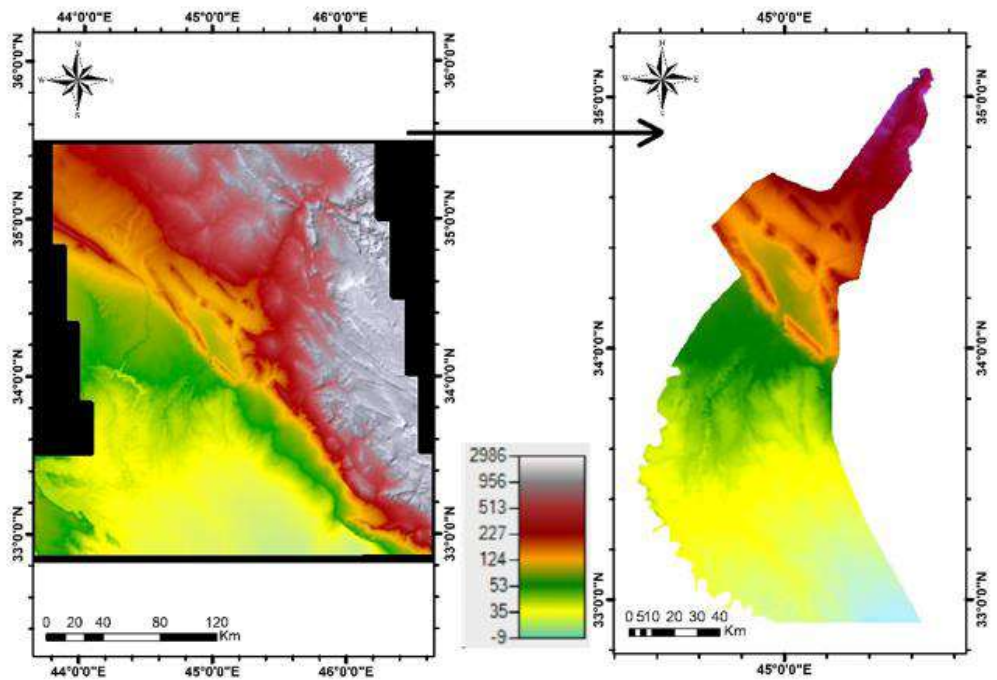


Figure 5.
Digital terrain model (DTM) of Study area.

3.3.2. Land Use & Land Cover (LULC) of Diyala River Basin

In this research, a land cover map with 10 m resolution was used. It is produced by Esri, Microsoft, and Impact Observatory in GeoTIFF format. It is derived from ESA Sentinel-2 imagery and is a composite of land use/land cover, available on <https://livingatlas.arcgis.com/landcoverexplorer/> (latest update 2023). The land cover map was imported into ArcGIS 10.5. The Manning roughness (n) polygon was created and then exported into the 2D model in HEC-RAS, and values of the Manning coefficient for each classified group depending on the classification and ID of every group, as illustrated in Table 1 and Figure 6.

Table 1.
Land cover classification with Manning's coefficient [30].

ID	Land cover classification	Manning's value
0	No Data	0.035
1	Unclassified	0.035
2	Developed – High intensity	0.15
4	Developed – Low intensity	0.1
5	Developed – Open space	0.04
7	Pasture / Hay	0.06
8	Grassland / Herbaceous	0.045
11	Mixed forest	0.08

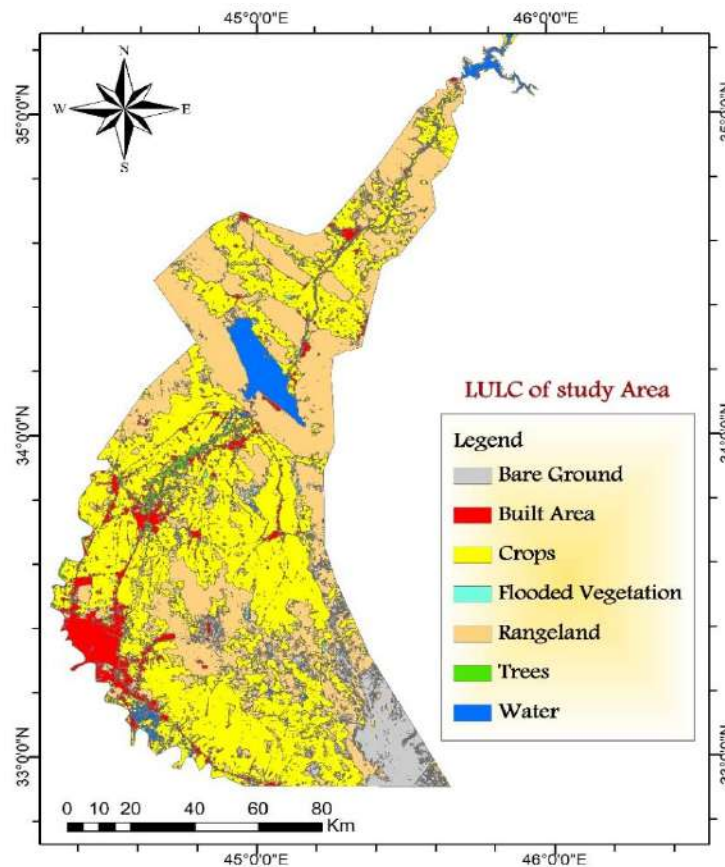


Figure 6.
Land use & land cover (LULC) of Study area.

3.4. Breach Parameter of Dam Collapse

Important factors are used in analyzing dam failure, but they cannot be predicted. The most important of these factors are the location of the breach, its size, and the time of its formation. There are a variety of special equations called regression equations that have been developed by previous researchers and are used to estimate breach parameters such as width, side slopes, volume eroded, etc., as well as the failure time. A dozen sets of predictive equations developed by various researchers to forecast breach geometry and outflow hydrograph parameters were compared [30, 31]. There is a large literature on the phenomenon of dam failure; this literature has discussed, developed, and used regression equations that are used to estimate breach parameters in the literature for the purpose of analyzing dam failures. The most important and widely used equations worldwide are Froehlich (1995a), Froehlich (2008), MacDonald and Langridge-Monopolis (1984), Von Thun and Gillette (1990), and Xu & Zhang (2009) [30-32].

These equations are implicit in the HEC-RAS software and are used to predict the breach parameters. Each scientist has their own set of empirical equations that figure out the values of the breach bottom width, the side slope, and the breach formation time based on what they know about how dams have failed in the past.

3.5. Initial and Boundary Conditions

In this research, the actual flows from Darbandikhan Dam, obtained from the Iraqi Ministry of Water Resources and shown in Figure 7, were used as upstream boundary conditions in model calibration and verification. The software used the breach outflow discharge hydrograph as upstream boundary conditions to simulate the resulting floods from the dam break. In both cases, the normal depth was adopted as downstream boundary conditions due to not knowing the true stage for the given flow at the downstream end of the model with a value of friction slope 0.002.

As for the initial condition, the water elevation equal to the dam crest elevation was considered an initial condition used in the reservoir, 495 m.a.s.l. overtopping case. At the same time, the initial water level was specified at terrain elevation as the initial condition for the downstream of the dam. Manning coefficient values were also calculated and inputted by adding "Land Cover map" (satellite image with TIF file type) to the model as an additional layer after it was obtained from the Esri database (latest update 2023), <https://livingatlas.arcgis.com/landcoverexplorer/>.

Enter Table Data time interval: 1 Day

Select/Enter the Data's Starting Time Reference

Use Simulation Time: Date: 11MAR.2019 Time: 24:00

Fixed Start Time: Date: 01MAR.2019 Time: 24:00

No. Ordinates Interpolate Missing Values Del Row Ins Row

Hydrograph Data			
	Date	Simulation Time (hours)	Flow (m3/s)
17	17Mar2019 2400	384:00:00	407
18	18Mar2019 2400	408:00:00	647
19	19Mar2019 2400	432:00:00	483
20	20Mar2019 2400	456:00:00	414
21	21Mar2019 2400	480:00:00	451
22	22Mar2019 2400	504:00:00	364
23	23Mar2019 2400	528:00:00	354
24	24Mar2019 2400	552:00:00	440
25	25Mar2019 2400	576:00:00	493
26	26Mar2019 2400	600:00:00	1016
27	27Mar2019 2400	624:00:00	830
28	28Mar2019 2400	648:00:00	738
29	29Mar2019 2400	672:00:00	853
30	30Mar2019 2400	696:00:00	750
31	31Mar2019 2400	720:00:00	740

Time Step Adjustment Options ("Critical" boundary conditions)

Monitor this hydrograph for adjustments to computational time step

Max Change in Flow (without changing time step):

Figure 7.
Upstream boundary condition of the model calibration and verification.

3.6. Flood Routing

There are two models in HEC-RAS, one dimensional (1D) model and two-dimensional (2D) model, where the HEC-RAS can simulate steady or unsteady flow by building them.

In the (1D) model, cross sections are created along river reach, which will be flood water path later, downstream the dam [33]. In the (2D) model, a grid composed of orthogonal cells is created to contain and represent the study area (As is the case in this research). The two-dimensional model allows water to flow in different directions. It will be a denser network representing the ground surface created by the grid, so the depth and velocity of water are simulated continuously [33]. HEC-RAS depends on the Shallow Water Equations (SWEs), which are called equation of Saint-Venant, also in performing the flood propagation model and finite volume method is used in 2D HEC-RAS models for solving the unsteady flow equations. As shown below, the Shallow Water Equations are represented by the continuity equation (mass conservation) and the momentum equations [30, 34].

Continuity equation (conservation of mass):

$$\frac{\partial h}{\partial t} + \frac{\partial q_x}{\partial x} + \frac{\partial q_y}{\partial y} = 0 \quad (1)$$

Momentum equation:

$$\frac{\partial q_x}{\partial t} + \frac{\partial}{\partial x} \left(u q_x + \frac{g h^2}{2} \right) + \frac{\partial}{\partial y} \left(\frac{q_x q_y}{h} \right) + g h (S_{fx} - S_{ox}) = 0 \quad (2)$$

$$\frac{\partial q_y}{\partial t} + \frac{\partial}{\partial y} \left(v q_y + \frac{g h^2}{2} \right) + \frac{\partial}{\partial x} \left(\frac{q_x q_y}{h} \right) + g h (S_{fy} - S_{oy}) = 0 \quad (3)$$

Where: h = water depth; t = time; x,y = space coordinate; q_x,q_y = river discharge in x,y direction respectively; u,v = velocity component in x,y direction respectively; g = gravity acceleration; S_{fx} , S_{fy} = friction term acting in the x,y direction respectively; S_{ox} , S_{oy} = bottom slope in the x,y direction respectively.

3.7. Calibration and Validation of the Model

For calibration and validation, satellite images of the land cover of the study area for a specific date were downloaded from the website (<https://earthmap.org/compare.html?geoJson/>). The inundation area map generated by RAS Mapper was converted to a shape file and output to ArcGIS software, and these shape files were then compared to different sections in satellite images along the river course in the study area with the same implementation date on the hydraulic model. Calibration and validation have been done for the information of 20/3/2019, and the results are accepted, as shown in Figures 8, and 9.

The selection of sites for calibration and verification purposes was random because the main objective of this procedure is to ensure that the model works correctly regardless of the locations of the selected places, as the selected sites, whether in the upper or lower part of the study area, are far from cities and are located in the open or between remote villages.

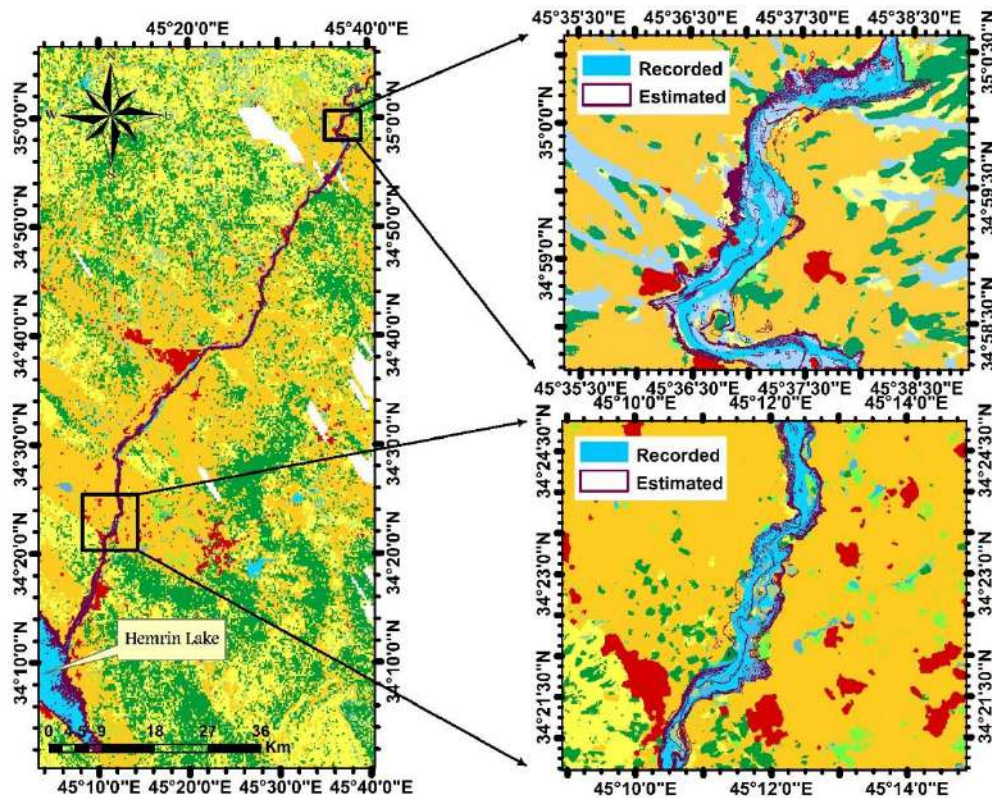


Figure 8.
Comparison at two locations along upper part of Diyala River.

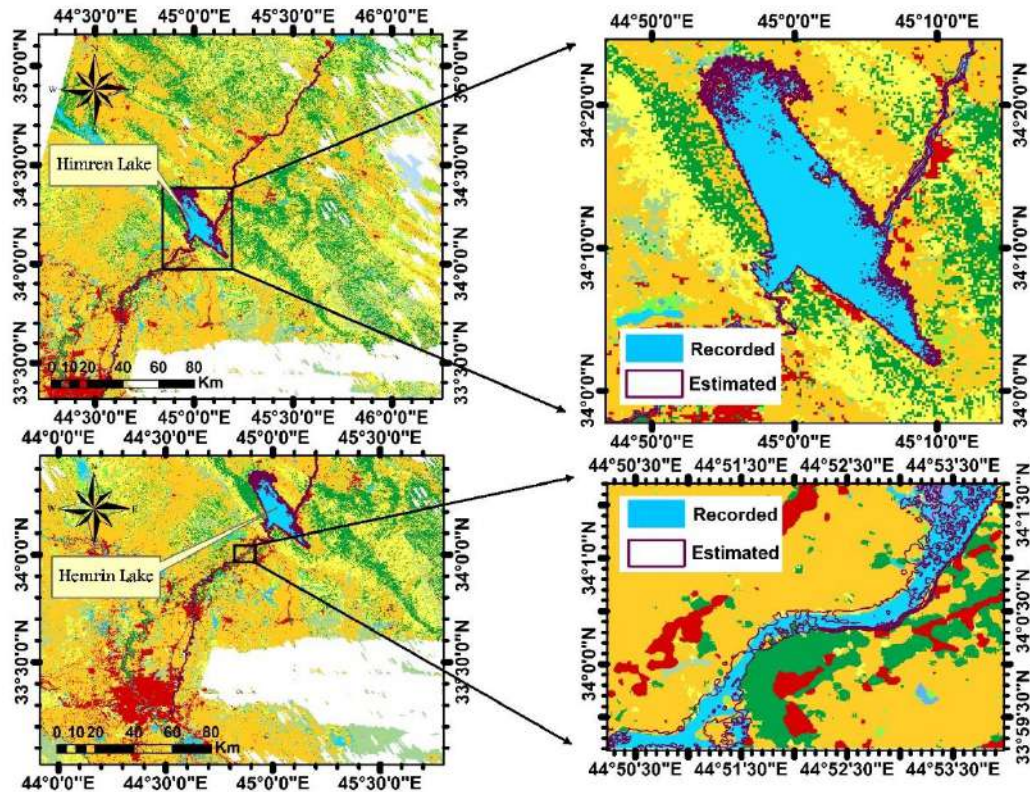


Figure 9.
Comparison at Hemrin Lake and one location on the lower part of the Diyala River.

3.8. Flood Mapping

In this section, the extent of the inundation maps is analyzed; the scenario used in this study is overtopping with the maximum storage elevation of the reservoir. Many factors are considered a measure of the severity of floods, especially floods that result from the collapse of dams, including the depth of the flood, the extent of the flooded area, the velocity of the flood, the damage factor (depth x velocity), and the warning time, in addition to other factors [35], where the modelling of the flood wave due to a dam break is considered one of the most unsteady flow problems that difficult to solve through HEC-RAS.

The RAS-Mapper is used to imagine the results in HEC-RAS and to show depth of water, water flow velocity, surface water level, and arrival time of the flood wave at every point inside the gridded polygon in the created terrain. Due to the extension of the study area in this research over a very wide area where the mesh of flow covers about (15525) Km², the network of flow area was used with a grid system consisting of cells with a size of (175 x 175) meters, resulting 501012 cells.

4. Results

4.1. Dam Break Analysis

To decrease the threat of flooding due to dam breaks, it is important to understand the flood characteristics of probable dam breaks in the true environment [36]. The worst scenario is considered the most useful for general planning purposes, which is a dam breaking when the reservoir is full [37]. The reservoir level was combined with a 12.5 m digital elevation model (DEM), where the water level of the reservoir at the moment of the dam breaking was considered 495 m.a.s.l., which is the elevation of the dam crest, and the spillway is considered blocked (the worst possibility), with the maximum capacity of the reservoir (4 x 10⁹) m³ [28]. The maximum outflow from the breach hole is approximately (381.1

$\times 10^3$) m^3/s , as shown in Figure 10. It takes approximately half a day for the reservoir to empty from water.

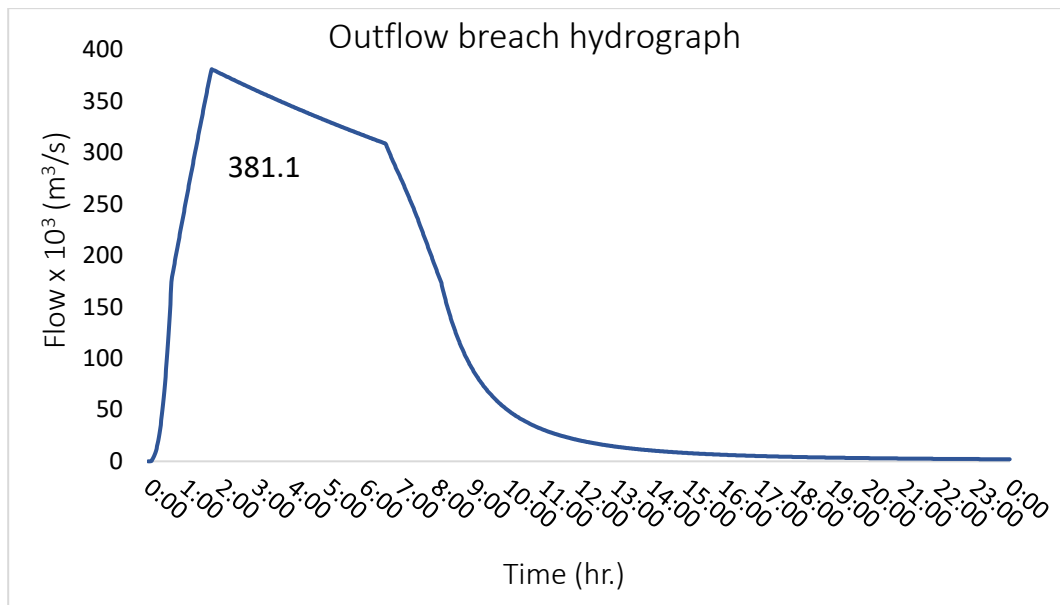


Figure 10. Outflow breach hydrograph of hypothetical break of Darbandikhan Dam.

4.2. Flood Extension and Topographic Analysis of the Study Area

As shown in Figure 11, the flood distribution never exceeds the outer boundary of the research area through the entire flood expansion process, which proves the research area setting rationality. The inundated lands are extending from the Darbandikhan Dam through Lake Hemrin and up to the Tigris River. Regarding the area of inundation in the study area, after implementing the inundation maps with the RAS- Mapper, these maps were exported to the Arc-GIS software to calculate the size of the inundation area in flood waters resulting from the hypothetical collapse of the Darbandikhan Dam. It was found to be approximately 8200 km², including the area of Lake Hemrin. The topography of the upper part is characterized by being a mountainous area, which leads to the confinement of flood waters in a narrow area along the course of the Diyala River. There are several cities and vital centers in the upper part of the Diyala River Basin, some of which are considered safe, such as Darbandikhan city center because it is in an area high above the river reach and Khanaqin city center because of its lateral location and it is far from the river reach in addition to some villages that far from the river path. Other places are within completely inundated areas, such as Sirwan district and other villages that are located near the river path. At the same time, there are other places exposed to partial inundation with different percentages, such as Kalar City, the district of Jalawla and Al-Saadiyah, and other villages. As for the lower part of the Diyala River, most of which is cultivated land all the way to Baghdad, the spread of the flood will be greater due to the flat nature of the land, where the flooded lands with vast areas, including most of the vital cities, such as Al-Muqdadiyah, Khalis, Baquba City (the administrative center of Diyala Governorate), Kanaan, and Baladrooz, in addition to most areas in the capital, Baghdad, especially the areas which is located east of the Tigris River, all the way to Al-Aziziyah city in north of Wasit Governorate towards the south.

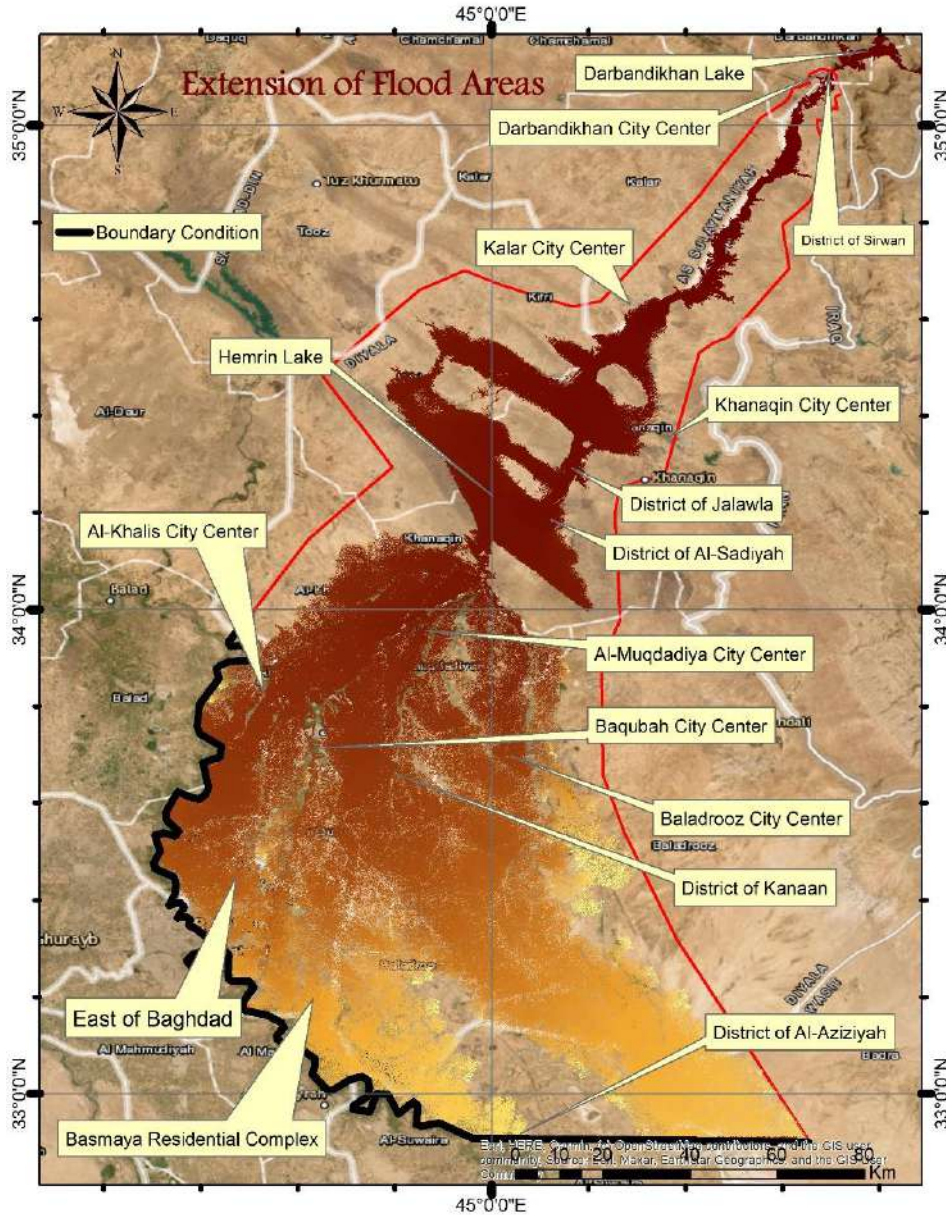


Figure 11.
Extension of flood areas inside the study area and the location of important cities

4.3. Parameters of Breach Hole

HEC-RAS software depends on the data related to the breach mode, the dam, and the reservoir (such as the height and crest width of the dam, water elevation in the reservoir, storage volume of the reservoir, and lateral slope of upstream and downstream of the dam) in modelling of breach development. Where the parameters of breach, such as the width of breach bottom, the breach side slope, and the time of breach formation, are extremely important in calculation the hydrograph of dam break outflow. Five methods were set to calculate the parameters of Darbandikhan Dam breach resulting from the various regression equations, as shown in Table 2.

As for choosing one of the equations, the (Von Thin and Gillette) equation is the most appropriate due to the dimensions of the dam from the foundation all the way to the crest, as the length of the dam at a level of 420 m.a.s.l (the level at which the storage of lake ends) is 270 meters [28], and the (Von

Thun & Gillette) equation is the only one among the equations in which the breach bottom width is less than 270 meters (205 meters). If another equation was chosen, the results would be illogical. Therefore, the results of the von Thun & Gillette equation will be adopted for the simulation process in this research.

Table 2.

The results of the breach parameters of Darbandikhan Dam resulting from the various regression equations.

Method	Mac Donald et al (1984)	Froehlich (1995)	Froehlich (2008)	Von Thun & Gillete (1990)	Xu & Chang (2009)
Breach bottom width (m)	1853	573	418	205	450
Side slope H: V	0.5	1.4	1	0.5	0.91
Breach development time (hrs)	8.27	6.4	4.73	1.75	9.26

4.4. Hydraulic Simulation (Flood Mapping)

One of the most important points that can be deduced from the hydraulic simulation of the flood resulting from the collapse of dams is determining the values and places of minimum and maximum limits for the depth, the velocity, the elevation, and the time of arrival of the flood water, in addition to knowing the propagation of the flood water in the area subject to flooding. The values of these data depend mainly on the dam-break flood hydrograph and its peak discharge, which is shown in Figure 10 according to a hypothetical break of the Darbandikhan dam. The peak flow rate reduces with the flood spread of the dam downstream [38, 39]. The results of the values of depths, speeds, and time of arrival of submerged water will be presented for specific cities characterized by their population density and the presence of administrative and service units therein when compared to other small villages close to them. From these cities: Darbandikhan city center, district of Sirwan, which is located less than 2 Km after Darbandikhan Dam, Kalar city center, Khanaqin city center, and the districts of Jalawla and Al-Saadiyah, this applies to the upper part of the Diyala Basin. In contrast, the lower part includes Al-Muqdadiya, Khalis, Baqubah, Baladrooz, and Kanaan, in addition to most of the cities of Baghdad which are located east of the Tigris River, all the way to Al-Aziziyah city in the north of Wasit Governorate towards the south.

4.4.1. Inundation Depths

The distribution and values of depths for the flood resulting from the hypothetical collapse of the Darbandikhan Dam can be seen in Table 3 and Figure 12, where depth maps are used to determine the extent of potential losses in areas exposed to the risk of flooding. The importance of the values of the upper limits is evident in the locations of cities and vital centers to estimate the amount of risk, where cities that are close to a dam or riverbed are the cities where the depths of flood water are greater. It is noted from Table 3 that the difference in the depth values for the upper part is greater compared to the depth values in the lower part, which explains the mountainous terrain and the strength of the flood wave in the upper part and the flat terrain and the reduction in the strength of the flood wave in the lower part.

Although Kalar City is closer to the Darbandikhan Dam than Jalawla City, the water depth in Jalawla City is greater because it is located in a low area on the riverbed, while the location of Kalar City is on the side of the river; this explains the danger of the location of cities on the riverbed, even if they are further from the dam than other cities.

The closer the city is to the river, the lower its level will be; it will be inundated under great water depths when exposed to the flood wave.

Table 3.

The hydraulic characteristics values of the flood due to the Darbandikhan Dam hypothetical break in the Diyala River Basin.

5	Jalawla	0 - 24	128 - 145	0 - 10	5.4 - 10.7	5
6	Al-Saadiyah	0 - 11	113 - 115	0 - 3.5	6 - 18	6
7	Al-Muqdadiyah	0 - 3.5	55 - 60	0 - 1.8	15 - 22	7
8	Baqubah	0 - 6	43 - 48.5	0 - 2.2	26 - 38	8
9	Khalis	0 - 2.5	43.5 - 48	0 - 2	27 - 50	9
10	Kanaan	0 - 3	44 - 46	0 - 0.6	31 - 41	10
11	Baladruz	0 - 1.9	40 - 41	0 - 0.5	36 - 63	11
12	East of Baghdad	0 - 3	33 - 38	0 - 1	39 - 110	12
13	Al-Aziziyah	0 - 0.6	21 - 22.6	0 - 0.3	169 - 186	13

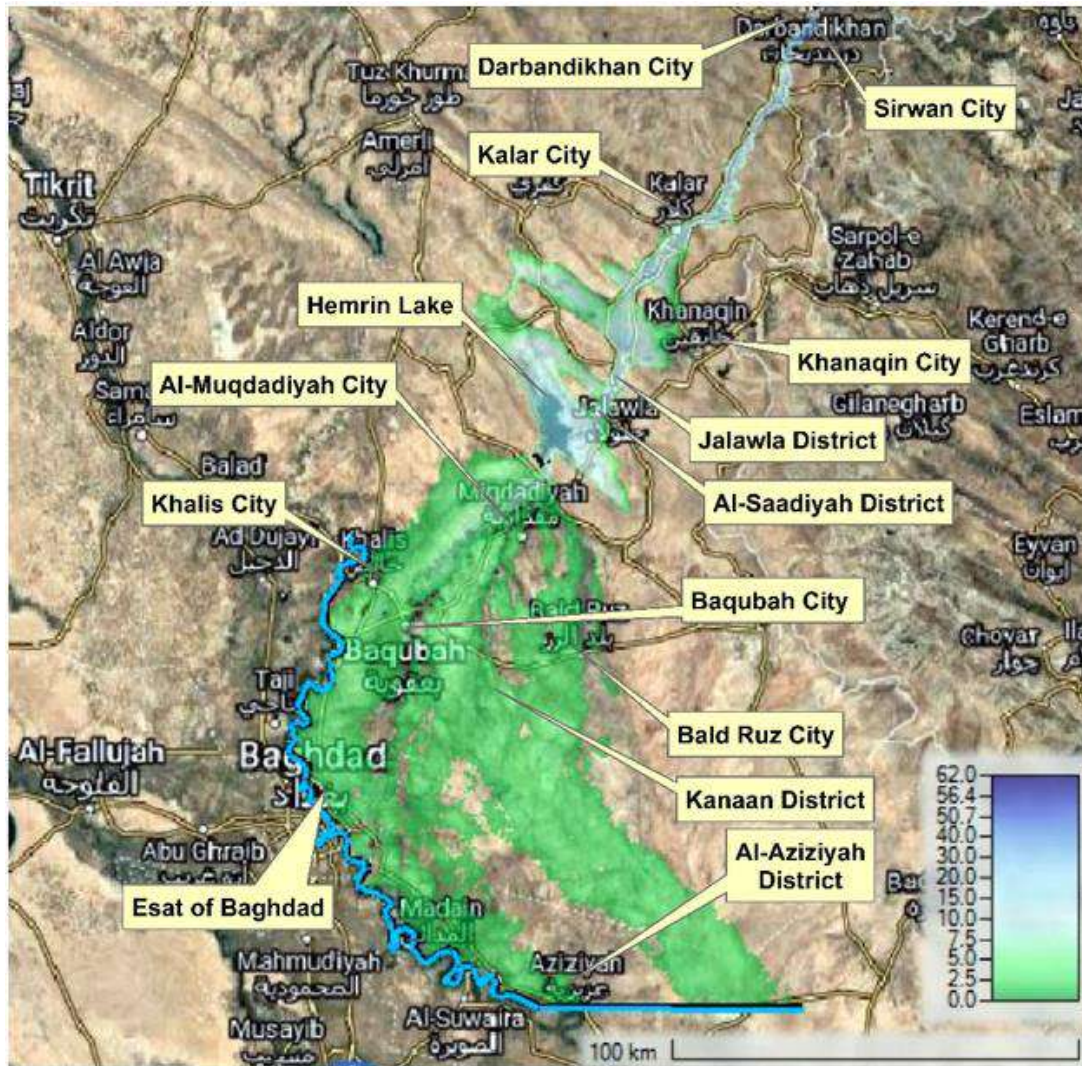


Figure 12.
Depths of inundation in the main and vital cities.

4.4.2. Inundation Velocity and Levels

The change in inundation water levels as it flows has an important impact on its velocity. Thus, the extent of the destruction and damage it causes to the lands through which it passes. The damage level is

classified by the depth and velocity values [40, 41]. The change in flood water levels is large, rapid, and sudden (i.e., the velocities are high) in the upper part of the Diyala River Basin, being a mountainous area. In contrast, in the lower part, the change in levels is gradual (i.e., the velocities are low); this means that the risk of erosion and sediment transfer in the upper part is greater than in the lower part. Table 3 represents the values of flood velocities and water surface levels that resulted from the Darbandikhan dam break, and Figures 13 and 14 represent the distribution of flood velocities and water surface levels, respectively.

It is noted that the flood wave velocity increases with the increase in the difference in water surface levels because it represents an increase in the slope of the region's terrain; this is clear when comparing flood velocities in the upper parts of the study area with the lower regions.

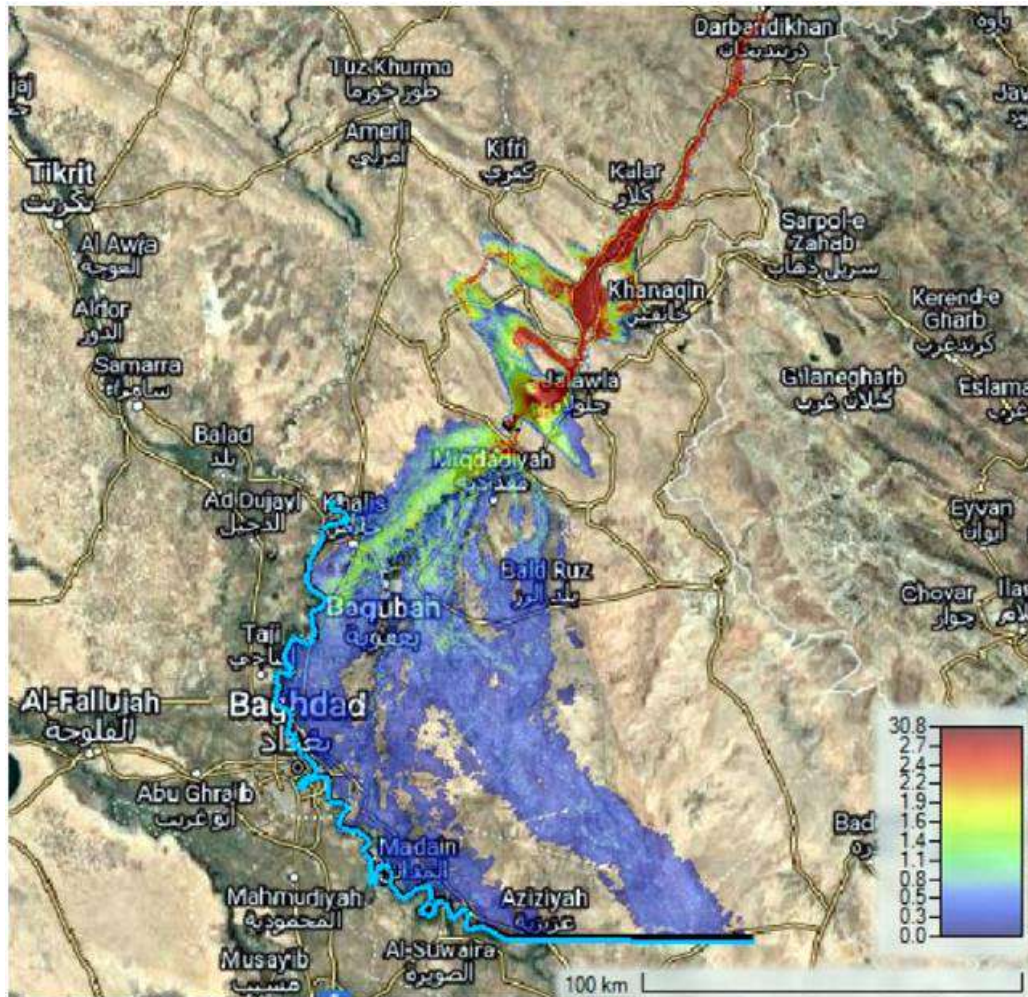


Figure 13.
Velocity of floods in the main and vital cities.

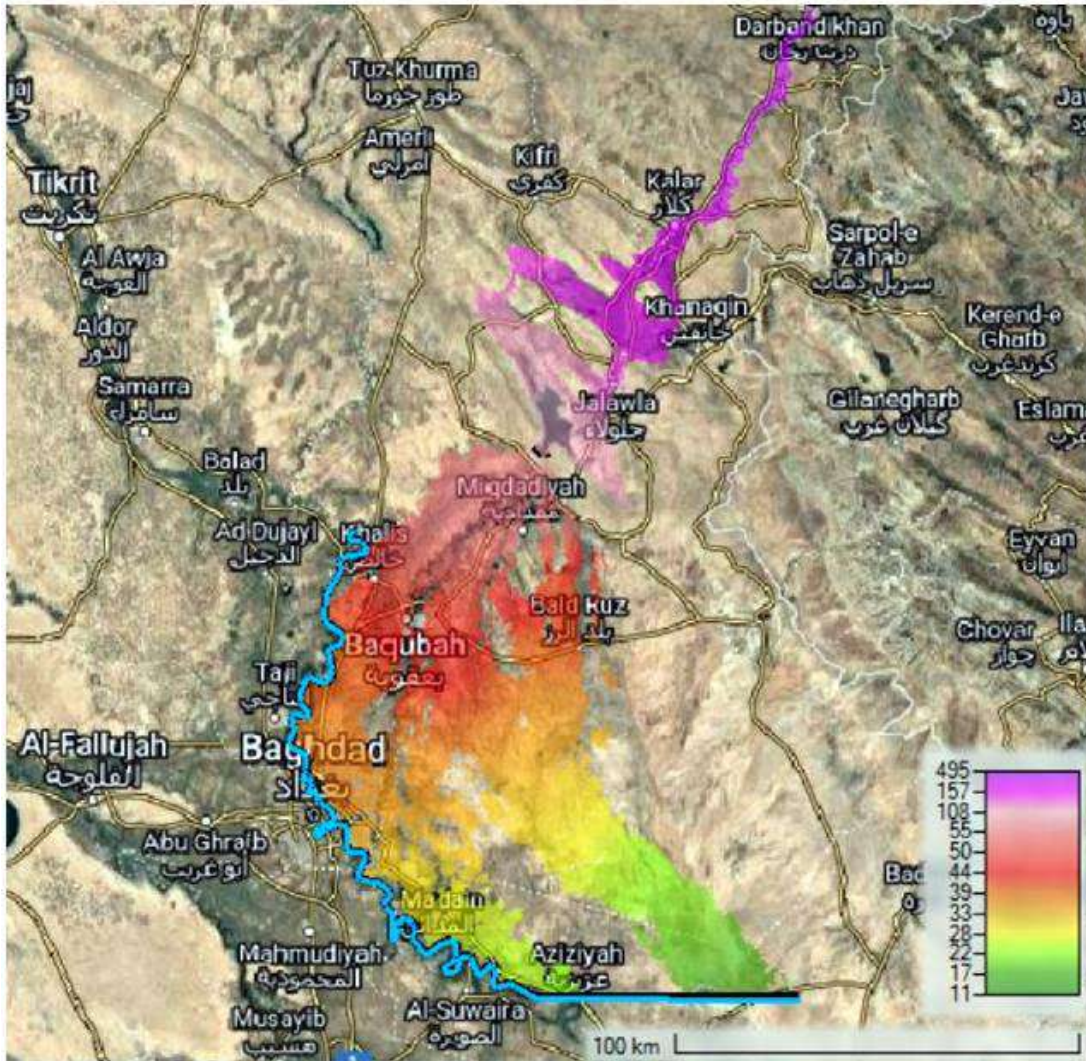


Figure 14.
Water surface level of inundation in the main and vital cities.

4.4.3. Flood Arrival Time

One of the most important main objectives of simulating floods resulting from the collapse of dams is to create an early warning system in addition to emergency plans by the concerned authorities. Still, there must be time available to benefit from early warning systems as well as to make emergency plans in proportion to the time available to implement those plans in if these floods occur, residents of cities near dams do not have enough time to take advantage of early warning systems or implement emergency plans. Thus, the lives of residents of those areas are more threatened than in areas that are farther from the dam, where the death rate increases the shorter the warning time. Among the results extracted from the process of simulating floods resulting from the collapse of dams are the arrival time of the flood wave in a specific area and the time of the development of the flood wave to its peak in the same area. For residents, the flood wave arrival time in their area of residence is considered more important than the peak time because the time of the arrival of the flood wave represents the time available to use roads before they are flooded, in addition to the possibility of other evacuation methods [42]. The breach start time is combined with the breach formation time to calculate the warning time, and then the time of the spread of the flood wave from the axis of the dam to a population center is

added, so the sum of what is mentioned is considered within the warning time [7]. Table 3 and Figure 15 illustrate the arrival time (by hours) of the flood due to the Darbandikhan dam virtual collapse through the study area. The HEC-RAS software can implicitly calculate the arrival time of a flood wave through the hydraulic model calculations of flood flow in the 2D flow area, and the arrival time is displayed as one of the model outputs.

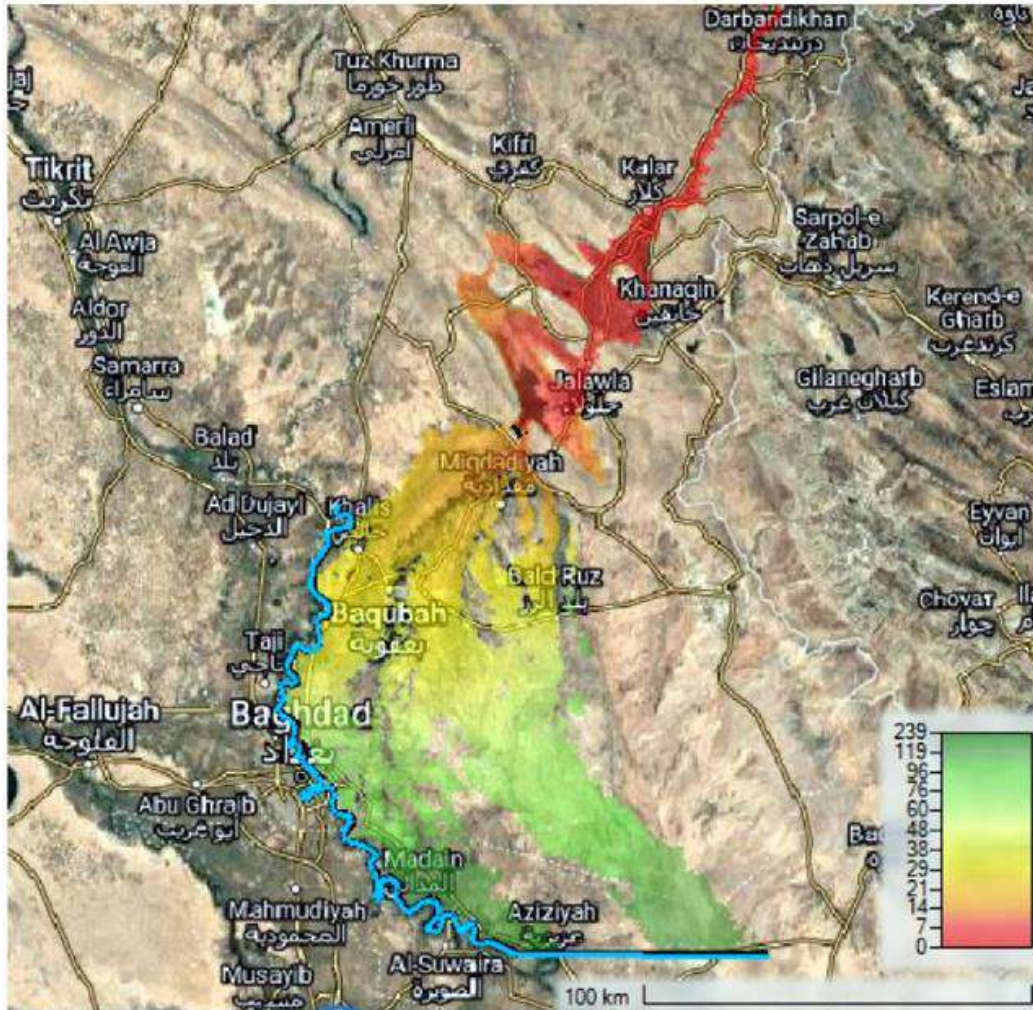


Figure 15. Arrival time of flood in the main and vital cities.

5. Conclusions

Failure of dams has many serious impacts. Accordingly, there is an urgent need to evaluate the damage caused by dam failure to develop plans that reduce the resulting losses. In this study, the resulting flood from the hypothetical break of Darbandikhan was simulated using a 2D HEC-RAS model, and it found the inundation area is 8200 km², including the area of Lake Hemrin. The values of depths and velocities of the flood wave decrease while the arrival time increases as one moves away from the dam towards the river reach, where the depths, velocities, and arrival time values in the closest city (Sirwan) are (17.5–58) m, (2–22) m/s, and (0.13–0.6) hours, respectively, while in the farthest city (Al-Aziziyah) are (0–0.6) m, (0–0.3) m/s, and (169–186) hours, respectively. The topography of the upper part of the Diyala River Basin is different, as it is a mountainous area with a steep slope, so the floods are of great depth and speed and are confined to a narrow area. The topography of the lower part is

characterized by flat lands with a slight slope, so the floods are of less depth and velocity compared to the upper part, and their spread is wider; this appears clearly in the inundation maps. Finally, It is important to take some measures, such as constructing a canal that connects the Hamrin reservoir down to a low-lying area to protect residents from the risk of flooding.

Author Contribution Statement:

Authors Isam Dhahir Khudhur and Ahmed Ahmed N. A. Hamdan: proposed the research problem.

Author Isam Dhahir Khudhur: developed the theory and performed the computations with the writing of the manuscript.

Author Ahmed Ahmed N. A. Hamdan: verified the analytical methods and investigated [a specific aspect] and supervised the findings of this work.

Both authors discussed the results and contributed to the final manuscript.

Copyright:

© 2024 by the authors. This article is an open access article distributed under the terms and conditions of the Creative Commons Attribution (CC BY) license (<https://creativecommons.org/licenses/by/4.0/>).

References

- [1] D. L. Fread, "BREACH, an erosion model for earthen dam failures," Hydrologic Research Laboratory, National Weather Service, NOAA, MD, United States, 1988, <https://www.rivermechanics.net/images/models/breach.pdf>
- [2] J. Mao, S. Wang, J. Ni, C. Xi and J. Wang, "Management system for dam-break hazard mapping in a complex basin environment," *ISPRS International Journal of Geo-Information*, vol. 6, no. 6, p. 162, 2017, <https://doi.org/10.3390/ijgi6060162>
- [3] C. Mattas, D. Karpouzou, P. Georgiou and T. Tsapanos, "Two-dimensional modelling for dam break analysis and flood hazard mapping: A case study of papadia dam, northern greece," *Water*, vol. 15, no. 5, p. 994, 2023, <https://doi.org/10.3390/w15050994>
- [4] R. Maddamsetty, T. V. Praveen, S. S. Rao and K. Manjulavani, "Tehri Dam-breach versus monsoon flood routing in the Ganga River system," *ISH Journal of Hydraulic Engineering*, vol. 16, no. 1, pp. 109-131, 2010, <https://doi.org/10.1080/09715010.2010.10514992>
- [5] FEMA, "Dam Safety: An Owner's Guidance Manual," Colorado Division of Disaster Emergency Services, Colorado, United States, 1987, Available: <https://www.fema.gov/emergency-managers/risk-management/dam-safety>
- [6] FEMA, "Federal Guidelines for Dam Safety," Federal Emergency Management Agency, united state, 2023, https://www.fema.gov/sites/default/files/documents/fema_rm-federal-guidelines-for-dam-safety.pdf
- [7] T. L. Wahl, "Uncertainty of Predictions of Embankment Dam Breach Parameters", *Journal of Hydraulic Engineering*, Vol. 130, no. 5, May 2004. ISSN 0733-9429 /2004/5-389-397; DOI:10.1061/(ASCE)0733-9429(2004)130:5(389)
- [8] ASDSO, "Incidents Search," 2020. [Online]. Available: <https://www.damsafety.org/incidents>
- [9] M. Cannata and R. Marzocchi, "Two-dimensional dam break flooding simulation: a GIS-embedded approach," *Natural Hazards*, vol. 61, no. 3, pp. 1143-1159, 2012, <https://doi.org/10.1007/s11069-011-9974-6>
- [10] S. Kumar, A. Jaswal, A. Pandey and N. Sharma, "Literature review of dam break studies and inundation mapping using hydraulic models and GIS," *International Research Journal of Engineering and Technology*, vol. 4, no. 5, pp. 55-61, 2017, https://scholar.google.com/scholar?hl=ar&as_sdt=0%2C5&q=Literature+review+of+dam+break+studies+and+inundation+mapping+using+hydraulic+models+and+GIS&btnG=
- [11] F. Xu, H. Zhou, J. Zhou and X. Yang, "A Mathematical Model for Forecasting the Dam-Break Flood Routing Process of a Landslide Dam," *Mathematical Problems in Engineering*, vol. 2012, pp. 1-16, 2012, <https://doi.org/10.1155/2012/139642>
- [12] A. El-Naqa and M. Jaber, "Floodplain Analysis Using ArcGIS, HEC-GeoRAS, and HEC-RAS in Attarat Um Al-Ghudran Oil Shale Concession Area, Jordan," *Journal of Civil & Environmental Engineering*, vol. 8, no. 5, pp. 1-11, 2018, DOI:10.4172/2165-784X.1000323
- [13] B. Balaji and S. Kumar, "Dam break analysis of Kalyani Dam using HEC-RAS," *International Journal of Civil Engineering and Technology (IJCIET)*, vol. 9, no. 5, pp. 372-380, 2018, https://iaeme.com/Home/article_id/IJCIET_09_05_041
- [14] E. Psomiadis, L. Tomanis, A. Kavvadias, K. X. Soulis, N. Charizopoulos and S. Michas, "Potential Dam Breach Analysis and Flood Wave Risk Assessment Using HEC-RAS and Remote Sensing Data: A Multicriteria Approach," *Water*, vol. 13, no. 3, p. 364, 2021, <https://doi.org/10.3390/w13030364>
- [15] A. Urzică, A. Miha-Pintilie, C. C. Stoleriu, C. I. Cimpianu, E. Huțanu, C. I. Pricop and A. Grozavu, "Using 2D HEC-RAS modeling and embankment dam break scenario for assessing the flood control capacity of a multi-reservoir system (NE Romania)," *Water*, vol. 13, no. 1, p. 57, 2021, <https://doi.org/10.3390/w13010057>

- [16] Bharath, A. V. Shivapur and C. G. Hiremath, "Dam break flood routing and inundation mapping using HEC-RAS and HEC-GeoRAS," in *Water Resources Management and Reservoir Operation: Hydraulics, Water Resources and Coastal Engineering*, Cham, Germany, Springer, 2021, pp. 129-137, https://doi.org/10.1007/978-3-030-79400-2_11
- [17] J. Y. A. Iroume, R. Onguéné, F. C. Djanna Koffi, A. Colmet-Daage, T. Stieglitz, W. Essoh Sone and J. Etame, "The 21st August 2020 flood in Douala (Cameroon): A major urban flood investigated with 2D HEC-RAS modeling," *Water*, vol. 14, no. 11, p. 1768, 2022, <https://doi.org/10.3390/w14111768>
- [18] Haltas, S. Elçi and G. Tayfur, "Numerical simulation of flood wave propagation in two-dimensions in densely populated urban areas due to dam break," *Water Resources Management*, vol. 30, pp. 5699-5721, 2016, <https://doi.org/10.1007/s11269-016-1344-4>
- [19] P. Mani, R. Kumar and J. P. Patra, "Dam Break Flood Hazard Assessment: A Case Study for a Small Dam at Source Stream of River Ganga in Uttarakhand, India," in *Roorkee Water Conclave*, Roorkee, India, 2020, https://www.iitr.ac.in/rwc2020/pdf/papers/RWC_188_Mani_et_al.pdf
- [20] T. M. Al-Taiee and M. S. Mustafa, "Hydrodynamic Simulation of Flood Due to Hypothetical Momentary Mosul Dam Failure," *Tikrit Journal of Engineering Sciences*, vol. 27, no. 4, pp. 48-57, 2020, DOI: <http://dx.doi.org/10.25130/tjes.27.4.06>
- [21] R. Karim, Z. F. Hassan, H. H. Abdullah and I. A. Alwan, "2D-HEC-RAS Modeling of Flood Wave Propagation in a Semi-Arid Area Due to Dam Overtopping Failure," *Civil Engineering Journal*, vol. 7, no. 9, p. 2021, 1501-1514, Doi: 10.28991/cej-2021-03091739
- [22] M. G. Tedla, Y. Cho and K. Jun, "Flood Mapping from Dam Break Due to Peak Inflow: A Coupled Rainfall-Runoff and Hydraulic Models Approach," *Hydrology*, vol. 8, no. 2, p. 89, 2021, <https://doi.org/10.3390/hydrology8020089>
- [23] Riswal, B. Sugiarto, M. Rifaldi and S. Zubair, "Flood Modelling Due to Dam Failure Using HEC-RAS 2D with GIS Overlay: Case Study of Karalloe Dam in South Sulawesi Province Indonesia," *Civil Engineering and Architecture*, vol. 10, no. 7, pp. 2833-2846, 2022, DOI: 10.13189/cea.2022.100704
- [24] F. S. Alrammahi and A. N. Ahmed Hamdan, "Hydraulic model for flood inundation in Diyala River Basin using HEC-RAS, PMP, and neural network," *Open Engineering*, vol. 14, no. 1, p. 13, 2024, <https://doi.org/10.1515/eng-2022-0530>
- [25] M. Al-Mukhtar and F. Al-Yaseen, "Modeling water quality parameters using data-driven models, a case study Abu-Ziriq marsh in south of Iraq," *Hydrology*, vol. 6, no. 1, p. 19, 2019, <https://doi.org/10.3390/hydrology6010024>
- [26] A. S. Khudier and A. N. A. Hamdan, "Assessment of the impacts of land use/land cover change on water resources in the Diyala River, Iraq," *Open Engineering*, vol. 13, no. 1, p. 20220456, 2023, <https://doi.org/10.1515/eng-2022-0456>
- [27] S. Khudier and A. N. A. Hamdan, "Hydrological Model of the Diyala River Watershed in Iraq Using Soil Water Assessment Tool," *Al-Bahir Journal for Engineering and Pure Sciences*, vol. 4, no. 2, p. 6, 2024, <https://doi.org/10.55810/2313-0083.1061>
- [28] SWLRI, "Strategy For Water And Land Resources In Iraq; Appendix G; Dams," Ministry of Water Resources of Iraq, Baghdad, Iraq, 2014.
- [29] F. S. Alrammahi and A. N. A. Hamdan, "Creating SCS curve number grid in Diyala river basin using land cover and soil data," in *AIP Conference Proceedings*, Melville, New York, 2023, <https://doi.org/10.1063/5.0140733>
- [30] G. W. Brunner, HEC-RAS River Analysis System 2D Modeling User's Manual, Davis, California, USA: US Army Corps of Engineers—Hydrologic Engineering Center (HEC), 2016, p. 1-171, <https://www.hec.usace.army.mil/software/hec-ras/documentation/HEC-RAS%205.0%202D%20Modeling%20Users%20Manual.pdf>
- [31] D. M. Gee, "Dam Breach Modeling with HEC-RAS Using Embankment Erosion Process Models," in *World Environmental and Water Resources Congress 2010: Challenges of Change*, Reston, Virginia, 2010, [https://doi.org/10.1061/41114\(371\)144](https://doi.org/10.1061/41114(371)144)
- [32] D. Z. Abdulrahman, "Case Study of the Chaq-Chaq Dam Failure: Parameter Estimation and Evaluation of Dam Breach Prediction Models," *Journal of Engineering Research and Applications*, vol. 4, no. 5, pp. 109-116, 2014, https://www.researchgate.net/profile/Kawa-Zaidan/publication/330117516_Case_Study_of_the_Chaq-Chaq_Dam_Failure_Parameter_Estimation_and_Evaluation_of_Dam_Breach_Prediction_Models/links/5c2e64ba458515a4c70a60c5/Case-Study-of-the-Chaq-Chaq-Dam-Failure-Parameter-Estimation-and-Evaluation-of-Dam-Breach-Prediction-Models.pdf
- [33] E. Ghimire, S. Sharma and N. Lamichhane, "Evaluation of One-Dimensional and Two-Dimensional HEC-RAS Models to Predict Flood Travel Time and Inundation Area for Flood Warning System," *ISH Journal of Hydraulic Engineering*, vol. 28, no. 1, pp. 110-126, 2022, <https://doi.org/10.1080/09715010.2020.1824621>
- [34] M. J. Mawat and A. N. A. Hamdan, "Simulation of 2D Depth Averaged Saint Venant Model of Shatt Al Arab River South of Iraq," *International Journal of Dynamics and Control*, vol. 18, no. 3, pp. 583-592, 2023, <https://doi.org/10.18280/ijdne.180310>
- [35] Australian Institute for Disaster Resilience, "Technical Flood Risk Management Guideline: Flood Hazard," Australian Disaster Resilience Handbook Collection, GUIDELINE 7-3 Australia, 2014, <https://knowledge.aidr.org.au/media/1891/guideline-7-3-technical-flood-risk-management.pdf>
- [36] M. S. Lodhi and D. K. Agrawal, "Dam-break flood simulation under various likely scenarios and mapping using GIS: Case of a proposed dam on River Yamuna, India," *Journal of Mountain Science*, vol. 9, no. 2, pp. 214-220, 2012, <https://doi.org/10.1007/s11629-012-2148-5>

- [37] Michaud, C. Johnson, J. Iokepa and J. Marohnic, "Methods for estimating the impact of hypothetical dam break floods," in *Chemistry for the Protection of the Environment 4*, New York, USA, Springer US, 2005, pp. 195-199, https://doi.org/10.1007/0-387-27448-0_17
- [38] S. E. Yochum, L. A. Goertz and P. H. Jones, "Case study of the Big Bay Dam failure: Accuracy and comparison of breach predictions," *Journal of Hydraulic Engineering*, vol. 134, no. 9, pp. 1285-1293, 2008, [https://doi.org/10.1061/\(ASCE\)0733-9429\(2008\)134:9\(1285\)](https://doi.org/10.1061/(ASCE)0733-9429(2008)134:9(1285))
- [39] Álvarez, J. Puertas, E. Peña and M. Bermúdez, "Two-dimensional dam-break flood analysis in data-scarce regions: The case study of Chipembe dam, Mozambique," *Water*, vol. 9, no. 6, p. 432, 2017, <https://doi.org/10.3390/w9060432>
- [40] H.-N. F. M. S. Committee, "Designing Safer Subdivisions," Hawkesbury-Nepean Floodplain Management Steering Committee, Parramatta, Australia, 2007, https://www.ses.nsw.gov.au/media/2249/subdivision_guidelines.pdf
- [41] "Hazard Classification in the US and Canada," 20 9 2022. [Online]. Available: <https://www.cityfloodmap.com/2013/12/flood-safety-guidelinesfor-depth-and.html>.
- [42] National Dam Safety, "Simplified Inundation Maps for Emergency Action Plans, National Dam Safety Review Board Emergency Action Plan Workgroup," 2009, <https://damsafety.org/sites/default/files/files/EAPWG%20Final%20SIMS.pdf>